SPECIAL PROJECT FINAL REPORT

All the following mandatory information needs to be provided.

Project Title:	Diabatic heating rates and moist tendencies along airstreams associated with different weather systems
Computer Project Account:	spchbojo
Start Year - End Year :	2021 - 2023
Principal Investigator(s)	Hanin Binder, Hanna Joos
Affiliation/Address:	ETH Zürich, Institute for Atmospheric and Climate Science, Zurich, Switzerland
Other Researchers (Name/Affiliation):	Dr. Franziska Aemisegger[1], Dr. Maxi Böttcher[1], Dr. Michael Sprenger[1],Dr. Leonie Villiger[1], Dr. Alexander Scherrmann[1], Dr. Emmanouil Flaounas[1], Franco Lee[1], Dr. Annika Oertel[2], Dr. Roman Attinger[3], Dr. Sophia Schäfer[4] 1) Institute for Atmospheric and Climate Science, ETH Zürich, Switzerland 2) Karlsruhe Institute of Technology, Karlsruhe, Germany 3) MeteoSwiss, Zurich, Switzerland 4) Météo-France

The following should cover the entire project duration.

Summary of project objectives

(10 lines max)

In this project we make use of our special IFS version that allows to output hourly all moisture, temperature and momentum tendencies from the parameterized physics. This model version has been used to simulate (i) a whole year (as part of the previous special project “Diabatic effects in mid-latitude weather systems”) and to (ii) perform case study simulations. With these simulations we analysed different aspects of the atmospheric moisture cycle and the impact of diabatic processes on extratropical dynamics, including (i) the moisture and heat budget of an extratropical dry intrusion into the North Atlantic trades, (ii) the moisture cycle in an extratropical cyclone, (iii) the occurrence of below-cloud cooling processes in the extratropics, (iv) the impact of diabatic processes on Mediterranean cyclones, and (v) a warm conveyor belt, (vi) the role of diabatic processes for the occurrence of clear air turbulence, and (vii) the importance of radiation for the formation of upper-level potential vorticity anomalies.

Summary of problems encountered

(If you encountered any problems of a more technical nature, please describe them here.)

In the last year of the project, we worked with Dr. Richard Forbes to implement the functionality of allowing additional output of momentum, temperature and moisture tendencies to the IFS CY47R3b version. Some compilation errors were encountered and significant residuals in the budget equations were present initially. Thanks to the great support by Dr. Richard Forbes, several trial forecast experiments have been performed, all compilation errors are solved, and the budget equations are closed. This special branch builds the basis for the ongoing special project “Diabatic processes and their impact on extratropical dynamics and the hydrological cycle”.

Experience with the Special Project framework

The application procedure for new special projects is very easy to follow as well as the progress reporting. We are very happy with the handling of all administrative aspects and also with the technical support.

Summary of results

The simulations which have been performed in the framework of this special project were essential for one dissertation about diabatic processes in Mediterranean cyclones and are used for one still ongoing dissertation about clear air turbulence. Furthermore, we made use of the simulations in our research-driven education of students which resulted in three Master theses. Additionally, a publication about the effect of the modification of potential vorticity by radiation is in preparation. The special project and the associated simulations are a key tool for the research in our team at ETH Zurich. In the following we will give a brief overview over all different projects.

1) Heat and moisture budget of an extratropical dry intrusion into the North Atlantic trades (Sara Müller, Dr. Franziska Aemisegger, Dr. Leonie Villiger, Dr. Maxi Boettcher)

Intrusions of dry upper-level extratropical air into the tropics play an important role in shaping the synoptic time-scale variability of the low-level cloud cover over the subtropical and tropical oceans (Aemisegger et al. 2021). An Integrated Forecasting System (IFS) simulation with heating rate and moist tendency output (0.4° horizontal resolution, 137 vertical levels) has been performed for an extratropical dry intrusion (EDI) reaching the Caribbean at the end of January 2018. The case has been studied extensively in a Master Thesis (Mueller, 2021). The three aims of this research are to

(1) analyse the heat and humidity budget along a North Atlantic EDI during its descent,
(2) quantify the impact of boundary layer clouds on the EDI's heat and moisture budget, and
(3) study the interaction of the EDI with the cold front and its impact on the cold front's southward propagation.

We therefore performed a detailed Lagrangian analysis of the EDI in the IFS simulation for the end of January 2018. During this period, the easterly trade winds were interrupted for several days by a coherent airstream consisting of rapidly descending air parcels reaching from the mid-latitude jet stream region into the sub-cloud layer in the trades. As those air parcels were anomalously dry and cold, they had a notable impact on diabatic processes in the vicinity of the trade-wind cloud tops such as primarily longwave cooling but also cloud evaporation and sublimation (Fig.1). To quantify the Lagrangian heat and moisture budget along the EDI, we analysed the individual diabatic heating rates (DHR) and moist tendencies (QVR) along Lagrangian trajectories based on hourly three-dimensional wind fields.

In the first part of their descent from the mid-tropospheric jet stream region, the EDI air parcels' heat budget is dominated by adiabatic warming of about 1 K h^{-1} and they conserve their initial upper tropospheric humidity (Fig. 1a,c). In the second part of their descent, they experience strong diabatic cooling of about -0.8 K h^{-1} and moistening at cloud tops of about 0.8 g kg h^{-1} (Fig. 1b,c).

The diabatic cooling is mainly due to radiative (-0.5 K h^{-1}) and microphysical processes (-0.3 K h^{-1}) and to a lesser extent due to turbulent cooling (-0.05 K h^{-1}). This diabatic cooling at cloud tops leads to cross-isentropic flow, which allows the EDI air parcels to pass through the inversion and to penetrate the boundary layer. Thereafter, the EDI air parcels experience strong diabatic warming by turbulent fluxes and shallow convection (by +0.2 to +0.5 K h^{-1}) in the lower part of the boundary layer. A net heating rate dipole is therefore experienced by EDI trajectories upon penetration into the boundary layer, with much larger prior cooling in regions with large cloud fractions than in regions with more scattered boundary layer clouds (not shown). The rapid diabatic warming in the boundary layer leads to a strong modification of the vertical structure of the cold front and to an erosion of the cold and dry anomaly in the lower free troposphere behind the southward propagating cold front.

The moistening of the EDI is primarily due to turbulent mixing (0.5 g kg h^{-1}) and convection (0.3 g kg h^{-1}) at cloud tops, while shortly after penetration into the boundary layer the EDI gets moistened about at equal rates by the large-scale microphysics scheme (cloud and precipitation evaporation) and turbulent mixing (0.25 g kg h^{-1}) (Fig. 1c). Within the boundary layer convection acts as a drying mechanism of EDI air parcels due to condensation in clouds and to convective mixing with the free troposphere (0.15 g kg h^{-1}).

In summary, this detailed EDI case study illustrates how the rapidly subsiding EDI airstream interacts with the parametrised subgrid-scale processes at cloud top in the model, thereby affecting the thermodynamic conditions in the boundary layer and impacting the southward propagation of the cold front.

Aemisegger, F., Vogel, R., Graf, P., Dahinden, F., Villiger, L., Jansen, F., Bony, S., Stevens, B., and Wernli, H.: How Rossby wave breaking modulates the water cycle in the North Atlantic trade wind region, Weather Clim. Dynam., 2, 281–309, https://doi.org/10.5194/wcd-2-281-2021, 2021.

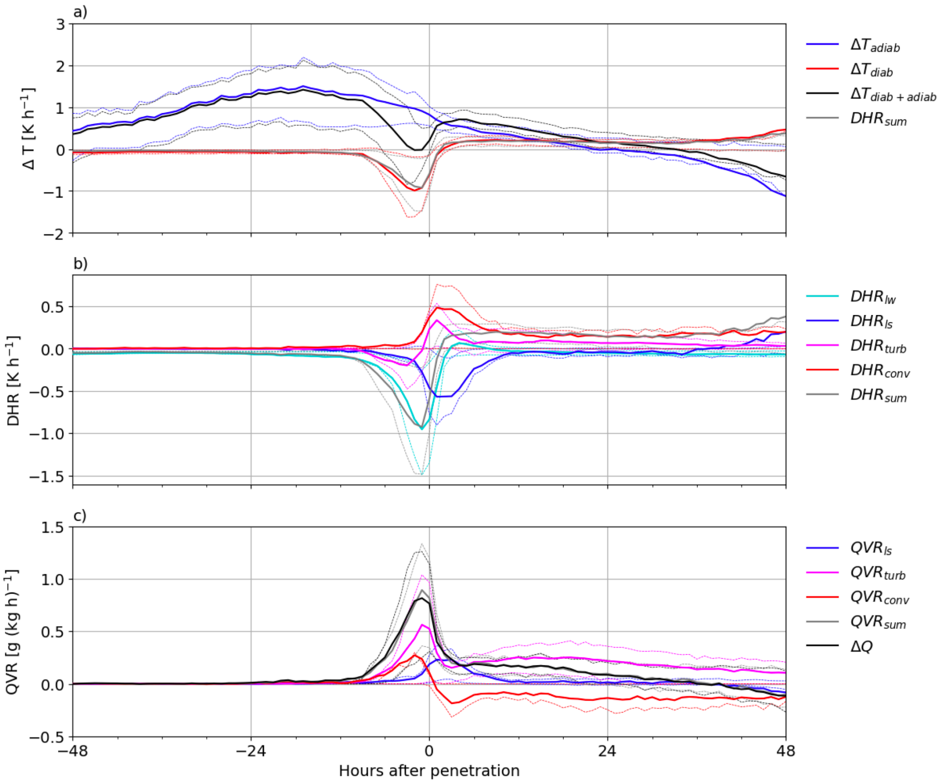

Fig. 1: Heat and water vapour budgets along the DI trajectories relative to their entry time into the boundary layer at *t*BLH in the time interval [*t*BLH -48 h, *t*BLH+48 h] for trajectories started at 00 UTC on 29 January. (a) Mean (thick lines) and 25th, 75th percentiles (thin lines) of the adiabatic (blue) and diabatic (red, grey) contributions to temperature changes along the trajectories as diagnosed from the thermodynamic energy equation applied to changes in T and q along the trajectories (red), sum of DHR from different processes (grey). (b) DHR from different processes parametrised in the model. The DHR from longwave radiation in cyan, from the large-scale microphysics in blue, from turbulence in pink, from convection in red, and the sum as in (a) in grey. The heating from shortwave radiation is small compared to the other processes and therefore not shown. (c) QVR from different processes in the model (same colours as in (b)).

2) Moisture cycle in an extratropical cyclone (Simon Eschle, Dr. Maxi Böttcher, Dr. Hanin Binder, Dr. Hanna Joos)

In a Master thesis (Eschle, 2022), the moisture sources and cycles of an extratropical cyclone have been investigated with data from an IFS simulation with hourly output of moisture tendencies from subgrid-scale processes (turbulence, convection and cloud microphysics) and from advection. The extratropical cyclone occurred in the North Pacific in April 2017. The goals of the thesis were to (1) determine the processes that were responsible for the moisture uptake in the cyclone, (2) identify the processes that moistened the airstreams around the cold front, (3) assess whether moisture recycling, i.e. the reuptake of moisture, occurred and (4) examine which role below-cloud processes (rain evaporation and sublimation of snow and ice) played. Lagrangian trajectories have been used to examine the pathways of air and moisture for a cross section through the cold front at the time of the strongest intensity of the cyclone.

It was found that advection, i.e. the transport of moisture, was the most important process leading to moisture changes (both moisture uptake and moisture loss) in different parts of the cyclone at the time of its strongest intensity. Turbulent processes were crucial for the uptake of moisture over the cold sector, whereas convection and large-scale cloud processes were mainly associated with moisture loss at the cold and warm fronts. The individual microphysical processes from the large-scale cloud scheme revealed that the moisture loss was mainly associated with condensation, followed by deposition of ice (Fig. 2a,b). At the same time, moisture uptake due to snow and ice sublimation and to a lesser extent due to cloud evaporation also played an important role at the cold and warm fronts (Fig. 2c-e). One dry intrusion airstream experienced moisture uptake through turbulent processes

This template is available at:
http://www.ecmwf.int/en/computing/access-computing-facilities/forms

when approaching the cold front. Two branches of the warm conveyor belt (WCB) were moistened by snow and ice sublimation at the cold front at the time of the strongest intensity of the cyclone. During the subsequent ascent, they experienced condensation and, later on, deposition of ice and snow. Air that was simultaneously moistened by rain evaporation and turbulence behind the surface cold front in the first place exhibited a WCB-like ascent afterwards. During its ascent, this air also encountered condensation. All these WCB and WCB-like airstreams partly revealed moisture recycling. During their ascents, liquid and ice clouds were formed by moisture originating from snow and ice sublimation or rain evaporation within the same cyclone. The results of this Master thesis highlight (i) the dominant contribution of advection to the moisture budget, (ii) the prominent role of snow and ice sublimation to the moisture budget and cycle, and (iii) that in this particular cyclone, moisture recycling was observed.

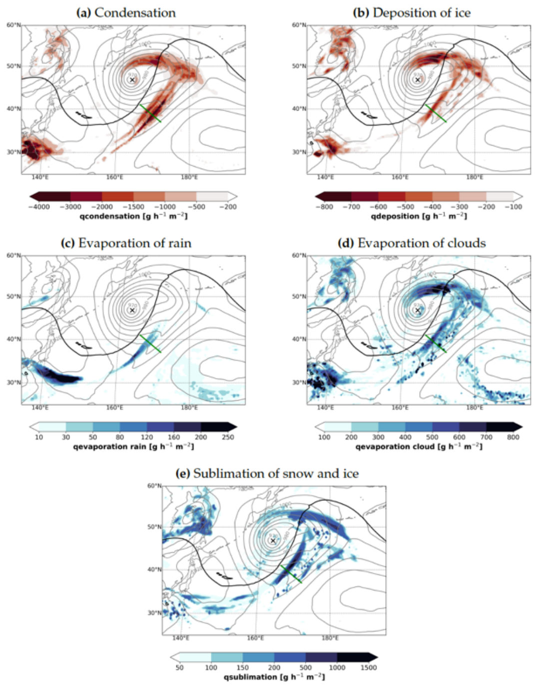

Fig. 2: Vertically integrated moisture tendencies (g h^{-1} m^{-2}; shading) of the individual microphysical processes from the large-scale cloud scheme at the time of the strongest intensity of the extratropical cyclone, at 17 UTC 10 April 2017. Shown are (a) condensation, (b) deposition of ice, (c) evaporation of rain, (d) evaporation of clouds, and (e) sublimation of snow and ice. Blue colours indicate regions with moisture uptake and red colours regions with moisture loss. Note that different colour scales are used for each tendency. In addition, the grey contours show sea level pressure (every 5 hPa) and the thick black line the 2 pvu contour at 320 K. The black cross marks the position of the cycle centre.

3) Emulating below-cloud cooling tendencies using random forests (Max Frei, Dr. Alexander Scherrmann, Dr. Hanna Joos)

In the Master thesis by Max Frei, we investigated where and how often below-cloud processes like sublimation or melting of snow, or evaporation of rain can lead to substantial cooling (and moisture supply) and consequently to PV modification in extra-tropical cyclones. We made use of the one-year IFS simulation from the previous special project, which provides hourly output of all physical tendencies, to find the regions in cyclones where cooling occurs. Based on the direct moisture tendency output, we trained a random forest which predicts where below-cloud cooling occurs based on relative humidity, the existence of snow and/or rain water, temperature, cloud cover and vertical velocity. The predictions are validated based on the 1-year IFS dataset which includes all cooling rates from the model output. The results from the random forest are shown in Figure 3.

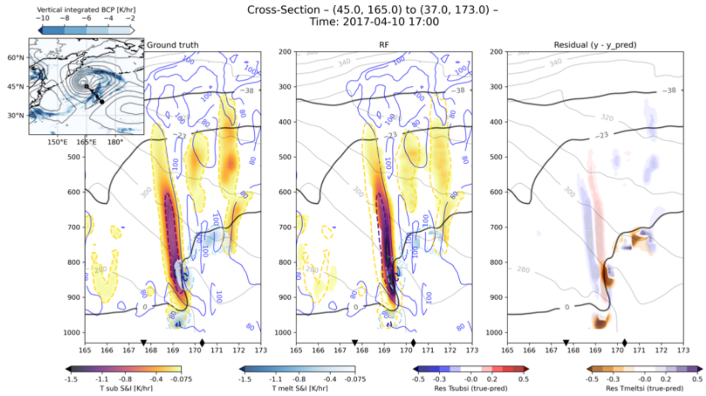

Fig. 3: Vertical cross section through a cold front. Cooling due to sublimation of snow and ice (yellow-purple colours, K h^{-1}), due to melting of snow and ice (bluish colours, K h^{-1}) from the IFS output (left panel) and the prediction from the random forest (middle panel). The right panel shows the difference in cooling rates between the IFS and random forest for cooling due to sublimation (red-blue colours, K h^{-1}) and due to melting (brown-blue colours, K h^{-1}).

In a next step, the random forest has been used to emulate the cooling due to evaporation of rain and sublimation of snow in ERA5 from 2012-2022. Evaporation of rain occurs mainly in the western parts of the north Atlantic and Pacific Oceans at the beginning of the strom tracks and the main starting regions of warm conveyor belts (Fig. 4).

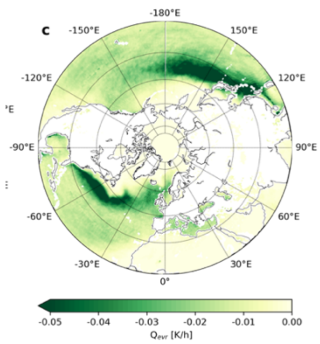

Fig. 4: Mean emulated cooling due to rain evaporation (colors, K h^{-1}) in ERA5 in the period from 2012-2022, vertically averaged from 850 to 1000 hPa.

4) Diabatic processes in Mediterranean cyclones (Dr. Alexander Scherrmann, Dr. Emmanouil Flaounas)

In the PhD project of A. Scherrmann, we investigated and quantified the PV modification by different diabatic processes in Mediterranean cyclones which are identified in the one-year simulation with the special IFS version. This simulation has been performed in the framework of the previous special project "Diabatic effects in mid-latitude weather systems". We combined the available PV tendencies with 48 hours backward trajectories (calculated using LAGRANTO) to (i) determine the most dominant diabatic processes in the Mediterranean basin that shape the lower-tropospheric PV anomaly found in Mediterranean cyclones, and (ii) determine where with respect to the cyclone centre the PV modification occurs, to define so called "cyclonic" and "environmental" PV with which we use to distinguish self- and remotely-driven cyclones and the dominant process inside and outside the cyclones. Figure 5 shows results obtained in step (i), where the PV modification accumulated along trajectories is shown as a distribution for all cyclones. Overall we find the main source of PV production to be dominated by convection (CONVT), turbulence (TURBM) and microphysics (MP), whereas turbulence (TURBT) and radiation (RAD) are the main source of PV destruction (Fig. 5a). Similar results were shown by Attinger et al. 2022 in North Atlantic extratropical cyclones. Splitting the contribution into its cyclonic and remote parts, Fig. 5b and c show that convection and microphysics are the main sources of PV production associated with the cyclone (Fig. 5b) and turbulence for the remote processes (Fig. 5c).

This template is available at:
http://www.ecmwf.int/en/computing/access-computing-facilities/forms

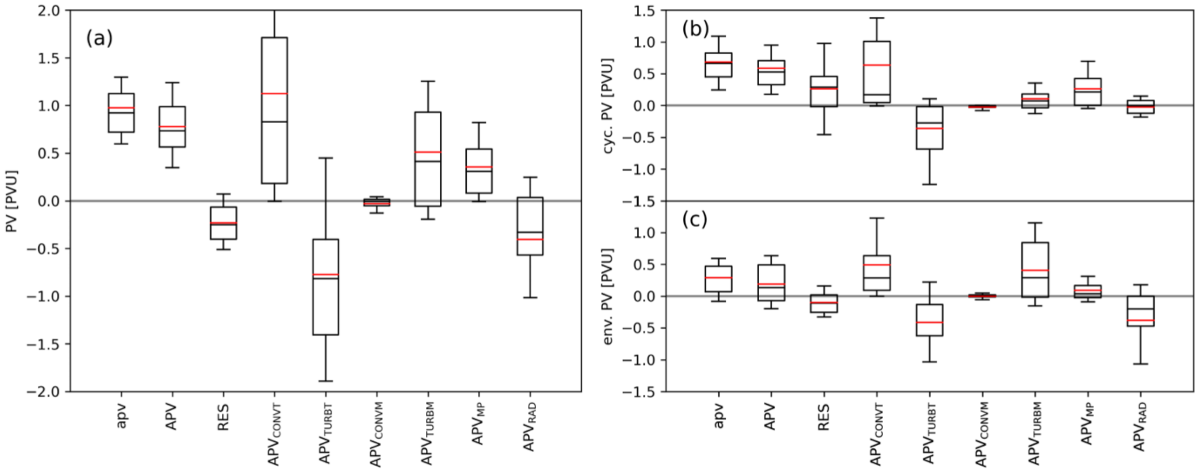

Fig. 5: Distribution of the average PV modification the Mediterranean cyclones experience due to diabatic processes along 48h backward trajectories initialized from the lower troposphere in the cyclone centre. (a): overall modifications; (b): modifications that are associated with processes occurring inside the cyclone; (c): modifications associated with remote processes outside the cyclone.

This work has been published in Weather and Climate Dynamics:

Scherrmann, A., Wernli, H., and Flaounas, E.: Origin of low-tropospheric potential vorticity in Mediterranean cyclones, Weather Clim. Dynam., 4, 157–173, https://doi.org/10.5194/wcd-4-157-2023, 2023

5) Diabatic heating and PV rates in a warm conveyor belt in the ICON and IFS model (Dr. Annika Oertel)

For the inter-model comparison of heating and PV rates from individual microphysical processes in WCBs in the IFS and ICON models, 4-day global free-running simulations of a WCB case study in October 2016 in the North Atlantic were conducted with the IFS and ICON models, respectively. The IFS is run at approx. 9 km horizontal grid spacing (TCo1279) and the ICON is run at a resolution of approx. 13 km (R3B07). Both simulations are initialized from the IFS analysis and remapped to a regular 0.2° x 0.2° grid. Trajectories are started in the North Atlantic region from an equidistant grid at seven vertical pressure and respective height levels in the lower troposphere.
While the simulations are quasi-identical at initialization, the larger-scale flow diverges substantially after 96 hours lead time. The comparison of WCB trajectories, defined as trajectories that ascend at least 600 hPa within 48 h, shows that in the IFS model the WCB trajectories do not only ascend faster on average (Fig. 6a), but also a substantially larger number of WCB trajectories is found in the IFS simulation. In total, more than twice as many WCB trajectories ascending in the entire North Atlantic region during the 4-day simulation are identified in the IFS model compared to the ICON model. Interestingly, WCB trajectories in the IFS on average descend before their fastest 600 hPa ascent, which is not represented in the ICON model, where trajectories remain below 900 hPa prior to their ascent. The diabatic heating during the ascent is comparable in both simulations and on average amounts to 23 K in ICON and 26 K in the IFS (Fig. 6c). WCB trajectories in the IFS reach a higher isentropic surface, due to their slightly higher diabatic heating and as they start their ascent at a higher isentropic surface.
Preliminary results show that the total hydrometeor content along the WCB ascent is larger in the IFS model, in particular during the rapid initial ascent phase (Fig. 6d). The separation into the individual hydrometeor types shows distinct differences in the detailed representation of the cloud structure, and between the separation in liquid and frozen hydrometeors. In the IFS simulation rain and snow water content are the dominant hydrometeor types, and both reach higher values than in the ICON model, where cloud water content reaches the highest values. Ice water content has similar values in both models and becomes most important in the WCB outflow region in the upper troposphere. Ongoing analysis will compare detailed diabatic heating and potential vorticity rates along WCB ascent, and

the influence of the different microphysical parameterizations on the cloud structure, heating patterns, and potential vorticity distribution.

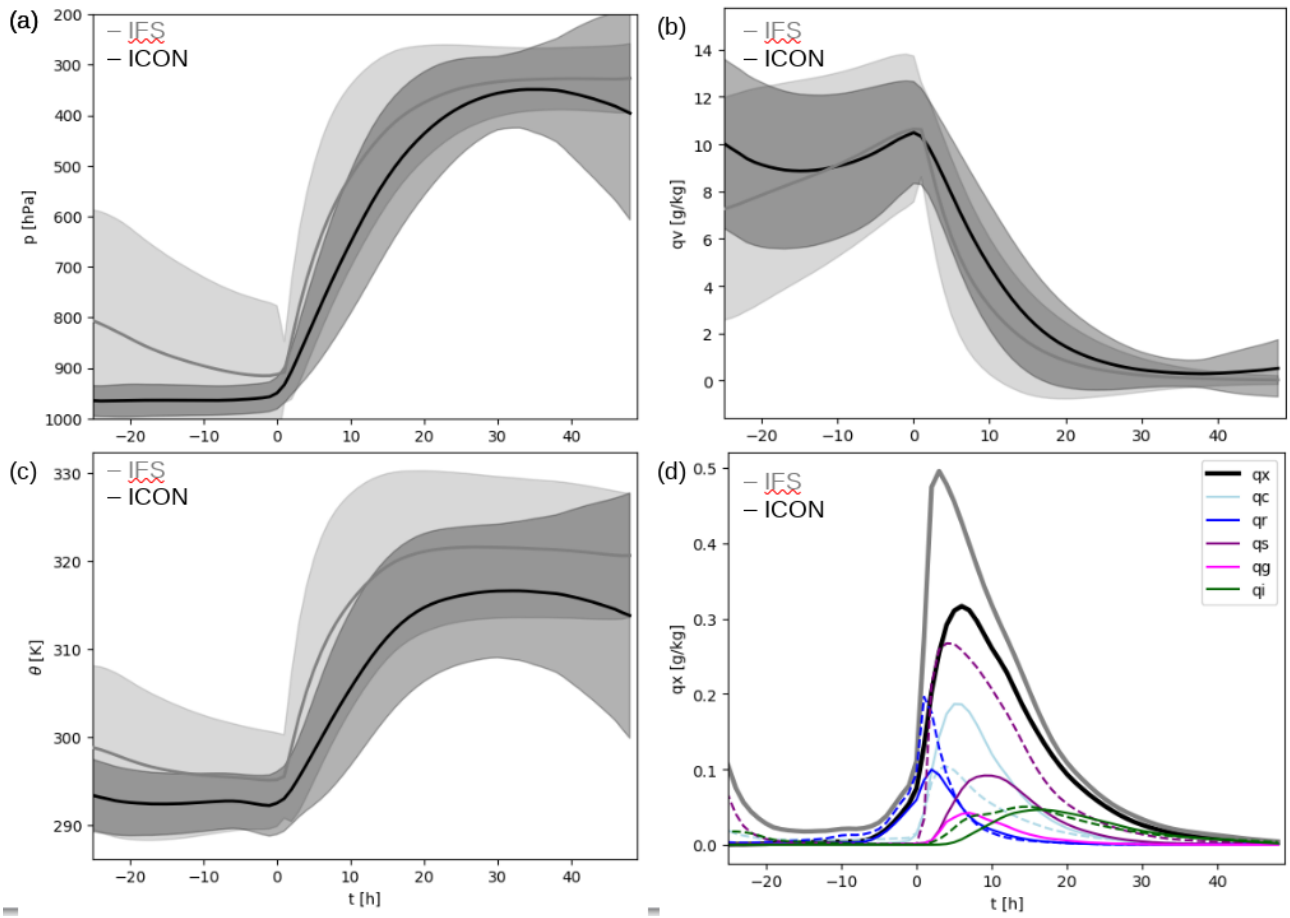

Fig. 6: Mean evolution plus standard deviation (shading) of (a) pressure (in hPa), (b) specific humidity (in g/kg), (c) potential temperature (in K), and (d) total hydrometeor content (g/kg) along WCB trajectories in the IFS (grey) and ICON (black) simulations. (d) additionally shows rain water content (qr, blue), cloud water content (qc, light blue), ice water content (qi, green), and snow water content (qs, purple) for the IFS (dashed) and ICON (solid) simulations. Graupel water content (qg, magenta) from the ICON simulation is also shown.

6) Clear air turbulence (Franco Lee, Dr. Michael Sprenger)

In the framework of this work package, the IFS version allowing for hourly output of all physical tendencies has been implemented to the model version CY47R3b. In autumn 2023, simulations of two case studies have been performed, one related to Rossby-wave breaking over the North Atlantic and one related to a warm-conveyor-belt outflow to the south of Japan. In Figure 7, the results of ECMWF's CAT diagnostic and a comparison to aircraft measurements of turbulence is shown.

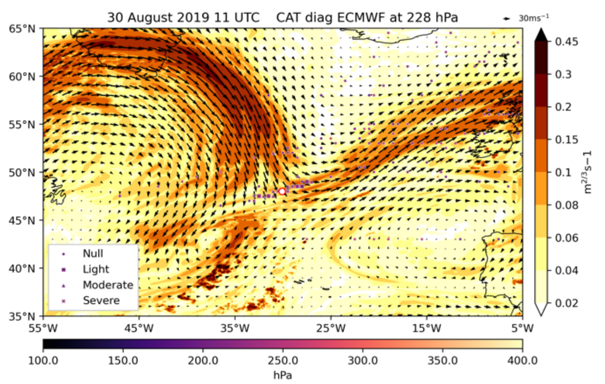

Fig.7: ECMWF's diagnostic of clear air turbulence at 228 hPa (colours) and aircraft measurements of null (circle), light (square), moderate (triangle) and severe (star) turbulence.

Both cases of clear air turbulence are further analysed in the ongoing special project “Diabatic processes and their impact on extratropical dynamics and the hydrological cycle”. The careful testing and analysis of the physical tendencies was essential, as this model version builds the basis for the projects in the ongoing special project. First results of the case study simulations are described in the progress report of the ongoing project.

7) Modification of potential vorticity by radiation in the extratropics (Noè Zardi, Dr. Roman Attinger, Dr. Sophia Schäfer, Dr. Hanna Joos)

We made use of the one-year IFS simulation, which has been performed in the framework of the previous special project “Diabatic effects in mid-latitude weather systems”, providing all physical tendencies with an hourly time resolution in order to investigate in which synoptic situations radiative temperature tendencies have the potential to modify potential vorticity (PV) substantially. We found that in the 6-month average, PV modification by longwave heating and cooling (especially in low levels) is of a similar magnitude as those from convection and turbulence. To investigate in more detail, we therefore selected two case studies where radiation contributed to the formation of (i) a positive PV anomaly in the lower troposphere which developed into an extratropical cyclone and (ii) an area with absolute negative PV close to the dynamical tropopause in an upper-level ridge. For both cases we could show that the shortwave and longwave heating as well as the longwave cooling leads to PV modification in a complex way. If these heating/cooling tendencies and the corresponding PV tendencies are accumulated along backward trajectories that originate from the considered PV anomalies, it can be seen that radiation can substantially modify PV as the air parcels experience this modification over several hours.
Figure 8 shows vertical time-height sections of the longwave heating/cooling rates (left) and the corresponding PV rate due to longwave heating (right) along trajectories ending in the upper-level negative PV region.

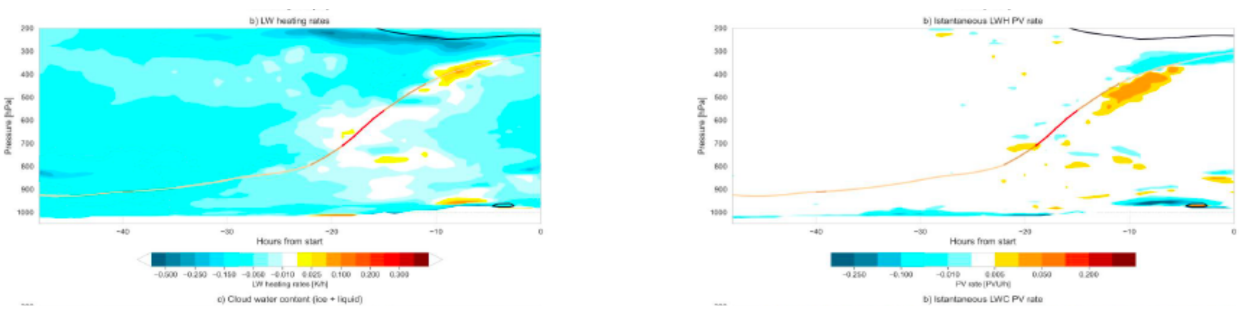

Fig. 8: Vertical time-height section along trajectories originating from an upper-level negative PV region. Colours denote the longwave heating/cooling rates (K h^{-1}) (left) and PV rates due to longwave heating (pvu h^{-1}) (right). The coloured line denotes the mean height of the considered trajectories coloured with their mean PV value (colourbar not shown). The black line denotes the 2 pvu-isoline.

It can be seen that trajectories ascend from the lower to the upper troposphere, whereas they do not experience PV modification due to radiation between -48h and ~-10h before they arrive in the upper troposphere. In the last ten hours before arrival PV is reduced, caused by the combination of longwave heating and cooling. PV is reduced above the heating maximum as well as below the cooling maximum. The trajectories therefore loose PV as they are traveling through this region and thus contribute to the formation of the absolute negative PV region. The accumulation of negative PV rates due to all radiative heating rates can also be seen in Figure 9. It shows that the PV values of the air parcels decrease between -0.5 and -1.5 pvu in 48h due to radiation.

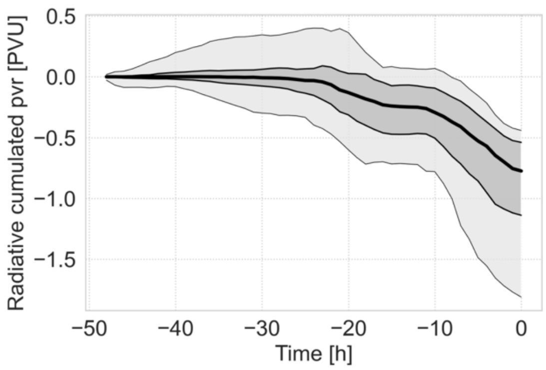

Fig. 9: Accumulated PV rates due to radiation (shortwave and longwave heating and longwave cooling) along 48h backward trajectories started from a region with absolute negative PV values in the upper troposphere.

List of publications/reports from the project with complete references

Eschle, S., Moisture cycle in an extratropical cyclone, MSc thesis ETH Zürich, 2022, supervised by M. Böttcher, H. Binder and H. Joos

Frei, M., Emulating below-cloud cooling tendencies using random forests: An analysis of extratropical cyclones in IFS and ERA5, MSc thesis ETH Zuerich, 2023, supervised by A. Scherrmann and H. Joos

Mueller, S., Diabatic processes associated with an extratropical dry intrusion reaching into the western North Atlantic trade wind region, MSc thesis ETH Zürich, 2021, supervised by F. Aemisegger, M. Boettcher and L. Villiger

Scherrmann, A., Wernli, H., and Flaounas, E.: Origin of low-tropospheric potential vorticity in Mediterranean cyclones, Weather Clim. Dynam., 4, 157–173, https://doi.org/10.5194/wcd-4-157-2023, 2023

Future plans

(Please let us know of any imminent plans regarding a continuation of this research activity, in particular if they are linked to another/new Special Project.)

The functionality of allowing additional output of momentum, temperature and moisture tendencies to the IFS CY47R3b version builds the basis for the ongoing special project "Diabatic processes and their impact on extratropical dynamics and the hydrological cycle", which started in January 2024. Based on this model version we plan to (i) simulate case studies of clear air turbulence (one case has already been simulated), (ii) simulate cyclones that are associated with sting-jets in a collaboration with Dr. Ambrogio Volonté from the University of Reading, (iii) perform case study simulations to investigate the moisture sources for warm conveyor belts and (iv) investigate the role of diabatic processes at the entrance of storm tracks for extratropical dynamics.